JOURNAL OF VIROLOGY, Apr. 2008, p. 3236–3249 Vol. 82, No. 7
0022-538X/08/$08.00+0 doi:10.1128/JVI.01887-07

The Fusion Protein of Respiratory Syncytial Virus Triggers p53-Dependent Apoptosis▽

Julia Eckardt-Michel,[1] Markus Lorek,[1] Diane Baxmann,[1] Thomas Grunwald,[2] Günther M. Keil,[3] and Gert Zimmer[1]*

Institut für Virologie, Zentrum für Infektionsmedizin, Stiftung Tierärztliche Hochschule Hannover, Bünteweg 17, D-30559 Hannover, Germany[1]; Abteilung für Mol. & Med. Virologie, Ruhr-Universität Bochum, Universitätsstrasse 150, D-44801 Bochum, Germany[2]; and Friedrich-Loeffler-Institut, Bundesforschungsinstitut für Tiergesundheit, Boddenblick 5a, D-17493 Greifswald-Insel Riems, Germany[3]

Received 29 August 2007/Accepted 13 January 2008

Infection with respiratory syncytial virus (RSV) frequently causes inflammation and obstruction of the small airways, leading to severe pulmonary disease in infants. We show here that the RSV fusion (F) protein, an integral membrane protein of the viral envelope, is a strong elicitor of apoptosis. Inducible expression of F protein in polarized epithelial cells triggered caspase-dependent cell death, resulting in rigorous extrusion of apoptotic cells from the cell monolayer and transient loss of epithelial integrity. A monoclonal antibody directed against F protein inhibited apoptosis and was also effective if administered to A549 lung epithelial cells postinfection. F protein expression in epithelial cells caused phosphorylation of tumor suppressor p53 at serine 15, activation of p53 transcriptional activity, and conformational activation of proapoptotic Bax. Stable expression of dominant-negative p53 or p53 knockdown by RNA interference inhibited the apoptosis of RSV-infected A549 cells. HEp-2 tumor cells with low levels of p53 were not sensitive to RSV-triggered apoptosis. We propose a new model of RSV disease with the F protein as an initiator of epithelial cell shedding, airway obstruction, secondary necrosis, and consequent inflammation. This makes the RSV F protein a key target for the development of effective postinfection therapies.

Respiratory syncytial virus (RSV) is the leading viral agent of lower respiratory tract disease in premature and young children but has been also recognized as an important pathogen for the elderly (23, 82), transplant recipients (3), and individuals suffering from cystic fibrosis (28, 85). Extrapulmonary manifestations of severe RSV infection have been reported as well (22). Immunity to RSV is incomplete and of short duration, allowing reinfections to occur throughout life (34). There is also evidence from experimentally infected mice that RSV is not always completely cleared from the lung and can persist in the respiratory tract (72). Infection with RSV may predispose children for asthma and airway hyper-responsiveness later in life (54, 74, 87).

RSV frequently induces severe respiratory disease associated with inflammation and obstruction of the small airways leading to dyspnea, wheezing, hypoxemia, and sometimes death (59). Important parameters leading to airway obstruction are smooth muscle contraction, edema formation, hypersecretion of mucus, and intense peribronchial infiltration of lymphocytes. In addition, RSV infection causes sloughing of ciliated epithelial cells, resulting in compromised pulmonary clearance and consequent secondary infections. Histological sections from RSV-infected patients revealed that the small bronchioles are often obstructed with plugs composed of mucus, fibrin, and desquamated epithelial cells (1, 42). The peripheral airways are disproportionately narrow prior to age five and are especially subject to obstruction (32, 41).

The fusion (F) protein of RSV is a trimeric transmembrane glycoprotein that mediates binding of RSV to cellular receptors and induces pH-independent fusion between the viral envelope and the cellular plasma membrane. The glycoprotein is also responsible for fusion of infected with adjacent cells, resulting in the formation of large multinucleated syncytia. Syncytium formation is associated with activation of RhoA, a small GTPase of the Ras superfamily (30, 64). Recent findings suggest that F protein induces proinflammatory cytokines, and this response is dependent on expression of pattern recognition receptors CD14 and TLR4 (51). Another intriguing feature of the F glycoprotein is the ability to inhibit mitogen-triggered T-cell proliferation by contact, a property that may contribute to immunosuppression (70).

The RSV F protein is an important antigen that induces virus-neutralizing antibodies, but for reasons that are not completely understood the antibody titers appear to be too low to provide sufficient protection (75). Despite many efforts, a licensed RSV vaccine is not yet available. Passive immunization with a humanized monoclonal antibody (palivizumab; Synagis) is the only approved prophylactic RSV therapy today for children at high risk. A therapy for acute RSV-induced bronchiolitis and disease is currently not available (63).

In this study, we demonstrate that RSV F expression causes p53-dependent programmed cell death leading to the loss of epithelial integrity and exfoliation of apoptotic cells from polarized epithelial monolayers. Based on these findings we hypothesize that the F protein plays an important role in airway obstruction and RSV-induced pathogenesis.

(This study was performed by J.E.-M. and M.L. in partial

* Corresponding author. Mailing address: Institut für Virologie, Zentrum für Infektionsmedizin, Stiftung Tierärztliche Hochschule Hannover, Bünteweg 17, D-30559 Hannover, Germany. Phone: 49 511 953 8460. Fax: 49 511 953 8898. E-mail: gert.zimmer@tiho-hannover.de.

▽ Published ahead of print on 23 January 2008.

fulfillment of the requirements for the Dr. rer. nat. degree at the University of Hannover, Hannover, Germany, 2008.)

MATERIALS AND METHODS

Cells and viruses. Madin-Darby canine kidney (MDCK) cells (type II) and HEp-2 cells were propagated in minimal essential medium containing 10% fetal calf serum (FCS). A549 cells were cultured with Dulbecco modified Eagle medium and 10% FCS. 16HBE14o immortalized human bronchial epithelial cells (37) were maintained in a mixture of Dulbecco modified Eagle medium and Ham F-12 medium supplemented with 10% FCS. The human RSV strains Long and A2 were gifts from Hans-Jürgen Streckert (University of Bochum, Bochum, Germany) and Geraldine Taylor (Institute of Animal Health, Compton, United Kingdom), respectively. The viruses were propagated on 16HBE14o cells and titrated as described previously (90).

Plasmids and inhibitors. The firefly luciferase reporter gene constructs p53-Luc, AP-1-Luc, TARE-Luc, and NF-κB-Luc were purchased from Stratagene. The plasmid p125-Luc with the firefly luciferase gene placed under control of an interferon-stimulated responsive element (86) was provided by Takashi Fujita (Department of Tumor Cell Biology, Metropolitan Institute of Medical Science, Tokyo, Japan). The plasmid pIRESneo-(p53-DN) encoding a dominant-negative p53 (R273H) was provided by Matthias Dobbelstein (Department of Molecular Oncology, University of Göttingen, Göttingen, Germany). The plasmid psiRNA-p53 driving the expression of p53-specific small hairpin RNA under control of the 7SK promoter and the control psiRNA-LucGL3 plasmid were purchased from InvivoGen.

All inhibitors were purchased from Merck Biosciences and were stored at −20°C as 1,000-fold-concentrated stock solutions in dimethyl sulfoxide.

Generation of stable transgenic cell lines. Codon-optimized open reading frames coding for F proteins of human RSV (Long strain; GenBank/EMBL accession number EF566942) (79), bovine RSV (49) (strain Stormond; accession number AM746678), and Sendai virus (strain Fushimi; accession number AM746621) were synthesized by GeneArt GmbH. Cloning of canine gp40/podoplanin cDNA was reported previously (91). The open reading frames were cloned into the pEGFP-N1 plasmid (Clontech) to generate chimeric proteins with the enhanced green fluorescent protein (GFP) at the respective C terminus. The chimeric genes were subcloned into the pGeneC expression vector (Invitrogen) and transfected into MDCK cells along with the pSwitch plasmid (Invitrogen). The transfected cells were grown for 14 days in selection medium containing hygromycin B (500 μg/ml) and zeocin (1 mg/ml). Cell clones were isolated by limiting dilution and analyzed for mifepristone-induced F-GFP expression by fluorescence microscopy and Western blotting. MDCK(hF-GFP) and A549 cells expressing dominant-negative p53 were generated by transfection of pIRESneo-(p53-DN) and selection with G418 sulfate (1 and 0.75 mg/ml, respectively). Control cells were transfected with nonrecombinant pIRESneo vector. A knockdown of p53 in A549 cells was achieved after transfection of the plasmid psiRNA-p53 and selection with zeocin (1 mg/ml). Zeocin-resistant cells were cloned by limiting dilution and analyzed by indirect immunofluorescence using an affinity-purified polyclonal antibody raised against full-length p53 of human origin (Santa Cruz Biotechnology). Cell clones showing the lowest p53 expression level were selected and used for infection studies. As a control, A549 cells were stably transfected with the psiRNA-LucGL3 vector expressing a randomized hairpin RNA.

Conditional antigen expression in polarized MDCK cells. MDCK cells were grown on 0.4-μm-pore-size, 6.5- or 24-mm-diameter Transwell polycarbonate filter supports (Costar) with daily changes of the cell culture medium. The transepithelial electrical resistance (TER) between the apical and the basolateral chamber was measured by using an ohmmeter (Millicell-ERS; Millipore). On day 3 or 4 after cell seeding the cells had usually formed a tight monolayer showing significant TER (>100 Ω cm^2). Transgene expression was induced by incubating the cells with mifepristone (10^{-9} M) for a maximum of 24 h. Inhibitors were added to the cells in some experiments as indicated and were renewed along with fresh medium on daily intervals. Floating cells in the cell culture supernatant were counted by using a Neubauer chamber.

Immunofluorescence and flow cytometry analysis. Transgenic MDCK cells were grown on either 6.5-mm-diameter porous polycarbonate filters for 3 to 4 days or 12-mm-diameter coverslips for 24 h before antigen expression was induced. The cells were fixed with 3% paraformaldehyde for 20 min and permeabilized with either 0.2% Triton X-100 for 5 min or cold (−20°C) methanol-acetone (1:2 [vol/vol]) for 1 min. Fixed cells were incubated for 60 min with either monoclonal antibody anti-β-catenin (clone 15B8, 1:500; Sigma), rabbit anti-Bax NH_2-terminus serum (N-20, 1:200; Santa Cruz Biotechnology) or rabbit anti-phospho-p53 (Ser15) serum (1:200; New England Biolabs), and antigens were visualized with either rhodamine-conjugated goat anti-mouse immunoglobulin G (1:500; Molecular Probes) or rhodamine-conjugated goat anti-rabbit immunoglobulin G (1:500; Dianova). In some experiments, nuclei were counterstained by incubating the cells for 15 min at 37°C with 0.1 μg of DAPI (4′,6′-diamidino-2-phenylindole; Sigma)/ml in methanol. Confocal laser scanning microscopy was performed by using a Leica LSM 2 microscope. Conventional epifluorescence was performed by using a Zeiss Axiovert 2 microscope.

For flow cytometry analysis, MDCK cells were grown on 24-mm-diameter polycarbonate filters for 3 to 4 days. At 24, 48, or 72 h postinduction of hF-GFP or SeV-F-GFP expression, the cells were detached from the filter supports using trypsin-EDTA solution, and GFP-positive cells were detected by using a Beckman-Coulter Epics XL cytometer equipped with Expo 32 ADC software. For detection of RSV infection by flow cytometry, A549 cells grown in six-well dishes were inoculated for 5 h at 37°C with human RSV (A2 or Long strain) using 3 PFU/cell. At 24 h postinfection, the cells were treated with accutase for 5 min at 37°C, collected by centrifugation, and incubated for 60 min at 4°C with a fluorescein isothiocyanate-conjugated bovine hyperimmune serum (1:100) that recognizes bovine, as well as human, RSV strains. In some experiments Synagis (5 μg/ml) was added to the cells at 8 h postinfection.

Cell surface labeling and immunoprecipitation. Transgenic cells were grown on 24-mm-diameter polycarbonate filter supports for 3 days before expression of hF-GFP or bF-GFP was induced. At 12, 24, 48, and 72 h postinduction the cells were labeled at the apical or basolateral domain with sulfo-NHS-LC-biotin (Pierce), and RSV F protein was isolated from the cell lysates by immunoprecipitation with monoclonal antibody RSV3216 (Serotec) as described previously (89). The immunoprecipitates were separated by sodium dodecyl sulfate-polyacrylamide gel electrophoresis, transferred to nitrocellulose membranes by semidry blotting, and incubated overnight with blocking reagent (Roche). After the membrane was incubated for 60 min with a biotinylated streptavidin-peroxidase complex (1:1,000; GE Healthcare), antigens were visualized by enhanced chemiluminescence (Super-Signal; Pierce). The light emission was recorded with a supercooled charge-coupled device camera (Chemi-Doc System; Bio-Rad) and quantified by using a densitometry software program (Quantity One; Bio-Rad).

Caspase assay. A549 cells and transgenic MDCK cells were seeded in 24-well plates (2×10^5 cells/well) and cultured for 24 h. A549 cells were infected with a multiplicity of infection (MOI) of 3 PFU/cell for 5 h at 37°C. MDCK cells received mifepristone (10^{-9} M) to induce hF-GFP expression. After incubation for 40 h in the presence or absence of indicated inhibitors, adherent cells were treated with trypsin, pooled with floating cells, pelleted by centrifugation, and resuspended in phosphate-buffered saline (PBS). To a 50-μl cell suspension containing 2×10^4 cells 50 μl of Caspase-Glo-3/7 reagent (Promega) was added, followed by incubation for 30 min at room temperature. The luminescence was measured by using a GeniusPro microplate reader (Tecan).

LDH assay. At 24 h after seeding of MDCK cells in 24-well plates (2×10^5 cells/well), the expression of hF-GFP was induced for 48 h. The release of lactate dehydrogenase (LDH) into the cell culture supernatant was determined by using the CytoTox-One homogenous membrane integrity assay (Promega) according to the manufacturer's instructions.

TUNEL assay. MDCK cells were grown on 12-mm-diameter coverslips for 24 h before the expression of hF-GFP or gp40-GFP was induced for 40 h. The cells were fixed with 4% paraformaldehyde for 1 h, permeabilized for 2 min on ice with 0.1% Triton X-100 in 0.1% sodium citrate, and incubated for 60 min at 37°C in the dark with 50 μl of TUNEL (terminal deoxynucleotidyltransferase-mediated dUTP-biotin nick end labeling) reaction mixture containing tetramethylrhodamine-dUTP and terminal deoynucleotidyl transferase (Roche Diagnostics). The samples were washed with distilled water and embedded in Mowiol prior to fluorescence microscopy.

Annexin V staining. A549 cells were grown in six-well plates (7×10^5 cells/well) and inoculated with RSV for 5 h using an MOI of 3 PFU/cell. At the indicated times, adherent cells were suspended by trypsin treatment and pooled with the cells that were floating in the cell culture supernatant. The cells were washed twice with cold PBS and resuspended in annexin binding puffer (Beckman-Coulter) to obtain a concentration of 10^6 cells/ml. To 100 μl of the cell suspension 10 μl of annexin V-phycoerythrin (PE) conjugate (Beckman-Coulter) was added, followed by incubation for 60 min at 4°C protected from light. The cells were pelleted by centrifugation, resuspended in PBS, and analyzed by flow cytometry (see above).

DNA laddering. Genomic DNA was extracted from 10^5 MDCK cells 40 h after induction of either hF-GFP or gp40-GFP expression by using a DNeasy tissue kit (Qiagen). The extracted DNA was separated by agarose gel electrophoresis and visualized by ethidium bromide staining.

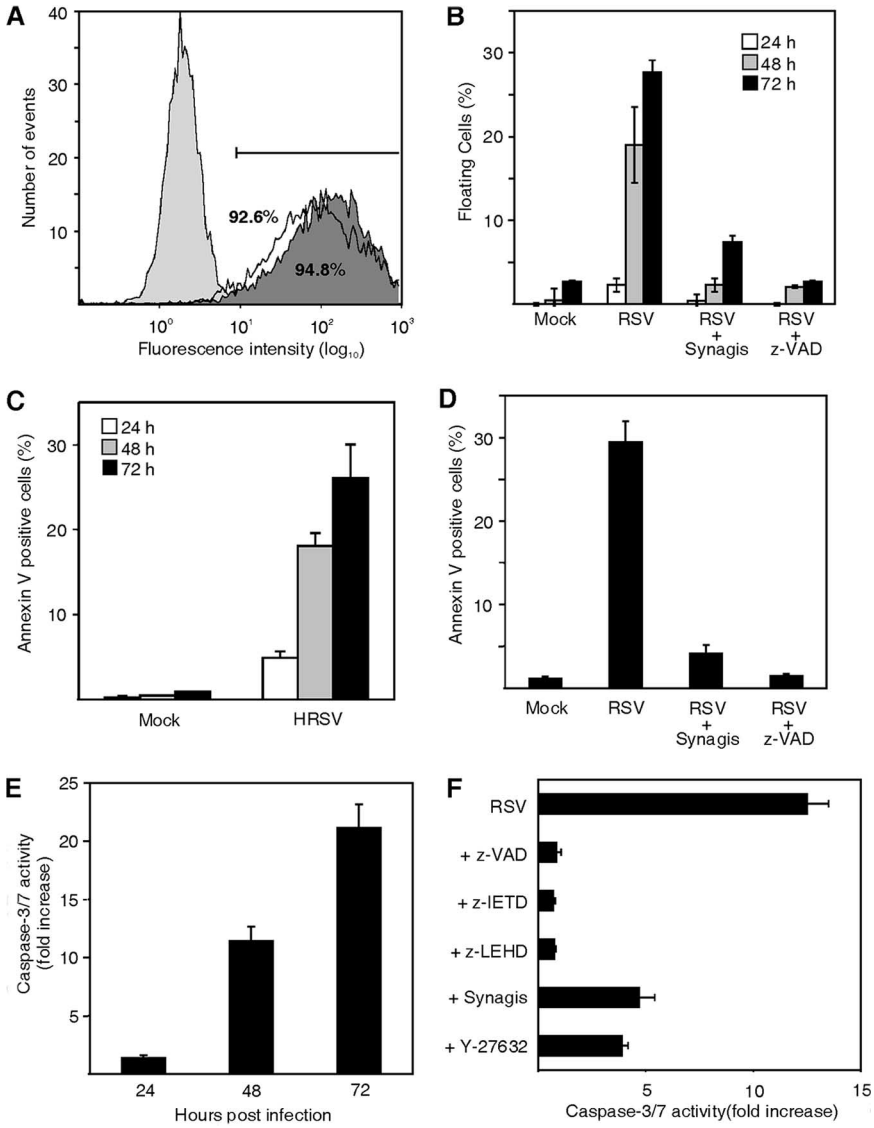

FIG. 1. Synagis inhibits apoptosis and shedding of RSV-infected A549 human lung epithelial cells. A549 cells were infected for 5 h with RSV A2 using 3 PFU/cell. (A) Flow cytometry analysis of A549 cells 24 h postinfection using an fluorescein isothiocyanate-conjugated polyclonal antiserum directed to RSV. The light gray and dark gray graphs represent mock-infected and RSV-infected cells, respectively. Cells that received Synagis (5 μg/ml) 8 h postinfection are represented by the white graph. (B) At the indicated times the cell culture medium was replaced, and the proportion of floating cells in the cell culture supernatant was determined. (C) Adherent and floating cells were pooled at the indicated times, and the percentage of cells that reacted with annexin V-PE was determined. (D) Synagis (5 μg/ml) and z-VAD (25 μM) were added to the cells 8 h postinfection. Adherent and floating cells were pooled 48 h postinfection and stained with annexin V. (E) At the indicated times, adherent and floating cells were pooled, and caspase-3/7 activity was determined in cell lysates. The relative fold increase in caspase-3/7 activity compared to mock-infected cells is shown. (F) At 8 h postinfection either Synagis (5 μg/ml), z-VAD pan-caspase inhibitor (25 μM), z-IETD caspase-8 inhibitor (25 μM), z-LEHD caspase-9 inhibitor, or Y-27632 Rho kinase inhibitor (5 μM) was added to the cells. At 40 h postinfection, caspase-3/7 activity was determined as described for panel E. The data represent the arithmetic means and standard deviations of three experiments.

Gene reporter assays. A549 or MDCK cells were seeded into 24-well cell culture plates (2×10^5 cells/well) and transfected with 1 μg of the respective luciferase reporter plasmid and 2 μl of Lipofectamine 2000 transfection reagent (Invitrogen). At 20 h posttransfection, A549 cells were infected with RSV A2 (3 PFU/cell) for 5 h, and MDCK cells received mifepristone (10^{-9} M) to induce hF-GFP expression. At 24 h, the cells were treated with trypsin, pelleted by centrifugation, and resuspended in PBS. Cell lysis buffer (100 μl; Promega) was added to 2×10^4 cells, and insoluble material was removed by centrifugation. To 20 μl of the clarified supernatant 80 μl of luciferase substrate was added (Luciferase Assay System; Promega), and luminescence was recorded by using a GeniusPro microplate reader.

RESULTS

Inhibition of RSV-induced apoptosis by F protein-specific antibody. As shown previously, A549 human lung epithelial cells undergo programmed cell death after infection with RSV (4, 50, 61). To study the effect of antibodies against the F protein on RSV-induced apoptosis, A549 cells were infected with RSV (A2 strain) using an MOI of 3 PFU/cell to ensure that more than 90% of the cells were infected (Fig. 1A). Al-

though no cytopathic effect was seen in mock-infected cells, some floating cells were already detected in the cell culture supernatant 24 h postinfection, and this effect became more dramatic at 48 and 72 h (Fig. 1B). When the pan-caspase inhibitor z-VAD was added 8 h postinfection, detachment of cells from the monolayer was almost completely abolished, indicating that caspase-dependent apoptosis was responsible for this effect. In apoptotic cells, phosphatidylserine is translocated from the inner to the outer leaflet of the plasma membrane, where it can be detected by annexin V conjugates (55). Mock-infected A549 cells did not react with PE-labeled annexin V (Fig. 1C), and only a small fraction of the cells (~5%) bound annexin V-PE when analyzed 24 h postinfection. However, about 20 and 30% of the infected cells were stained with annexin V-PE at 48 and 72 h postinfection, respectively. In the presence of the pan-caspase inhibitor z-VAD apoptosis was suppressed and infected cells did not react with annexin V-PE (Fig. 1D). In line with these findings, caspase-3/7 activity was rather low at 24 h postinfection but high at 48 and 72 h (ca. 10- and 20-fold increases, respectively, Fig. 1E). The addition of z-VAD reduced caspase-3/7 activity to background levels (Fig. 1F). Specific inhibitors of the initiator caspase-8 (z-IETD) and caspase-9 (z-LEHD) were equally effective, suggesting that the extrinsic and intrinsic pathways act in concert during RSV-induced cell death. An inhibitory effect was also accomplished by the Rho kinase inhibitor Y-27632, suggesting that RhoA signaling is involved in RSV-triggered apoptosis. Synagis, a humanized monoclonal antibody directed against the RSV F protein that blocks virus entry by interfering with the fusion activity of the protein, did not inhibit infection when given 8 h postinfection (Fig. 1A) but significantly protected A549 cells from apoptosis (Fig. 1B,D). Accordingly, Synagis reduced caspase-3/7 activity in RSV-infected cells, albeit with lower efficacy than z-VAD (Fig. 1F). Similar results were obtained with the Long strain of RSV (data not shown). These data suggest that the F protein plays an important role in RSV-induced apoptosis.

RSV F expression affects epithelial integrity. To study the impact of RSV F protein expression on polarized epithelial cells in the absence of virus replication and other RSV proteins, we generated stable MDCK cell lines that expressed either the human or the bovine RSV F protein in a regulated manner. GFP was linked to the viral glycoproteins at their cytoplasmic domains to ease detection. The cells were grown on porous filter supports for 3 to 4 days to allow formation of a polarized epithelial monolayer before RSV F protein expression was induced. Confocal laser scanning microscopy revealed that the human RSV F protein (hF-GFP) was predominantly transported to the apical plasma membrane, whereas β-catenin, a cellular protein, was exclusively found at the basolateral plasma membrane, indicating that the cells were still polarized at 12 and 24 h postinduction. However, when hF-GFP was expressed for more than 24 h, the strictly polarized distribution of the protein was significantly affected (Fig. 2A, upper panel). The typical columnar morphology of the epithelial cells changed to an irregular and flattened shape, and several cells were found to be extruded from the apical site of the monolayer (indicated by arrows). An even more pronounced cytopathic effect was mediated by the bovine RSV F protein (Fig. 2A, central panel), whereas MDCK cells did not reveal any morphological changes for the whole time of analysis when a cellular glycoprotein fused to GFP (gp40-GFP) was expressed under the same conditions (Fig. 2A, lower panel). Like RSV F protein, gp40 is a type I membrane protein that is targeted to the apical plasma membrane domain of polarized MDCK cells (91).

To confirm the immunofluorescence data, we took advantage of a membrane-impermeable biotinylation reagent to selectively label the cell surface proteins of filter-grown MDCK cells at either the apical or the basolateral domain. A characteristic pattern of apical and basolateral proteins was detected in whole-cell lysates 12 and 24 h after induction of hF-GFP expression confirming that the cells were polarized (Fig. 2B, lower panel, 12 and 24 h). However, prolonged expression of hF-GFP (48 and 72 h) abrogated the asymmetric distribution of cell surface proteins, indicating that cell polarity was significantly affected at this time. In addition, the pattern of biotinylated proteins looked different at 48 h compared to 12 or 24 h. This phenomenon may be attributed to apoptosis (see below), leading to proteolysis of cell surface proteins and/or changes in the protein pattern of the cell surface. Immunoprecipitation of biotin-labeled hF-GFP revealed that the protein was predominantly located at the apical membrane 12 and 24 h after induction (Fig. 2B, upper panel), whereas a significant portion of the protein (37%) was found at the basolateral membrane 48 h postinduction. Less F antigen was detected at 72 h, probably due to the loss of epithelial cells (see below). Likewise, the bovine RSV F protein (bF-GFP) was predominantly expressed at the apical plasma membrane but, in contrast to hF-GFP, a significant amount of bF-GFP could be also detected at the basolateral membrane early after induction. At 72 h, similar levels of bF-GFP were biotinylated at the apical and basolateral membranes, indicating that cellular polarity was completely lost (Fig. 2B, second panel).

The most striking consequence of RSV F protein expression in polarized MDCK monolayers was the loss of epithelial cells. Already 24 h postinduction of hF-GFP expression, numerous floating cells were detected in the apical cell culture supernatant and this effect increased until 72 h (Fig. 3A). Cell detachment was more prominent with MDCK cells expressing bF-GFP, indicating that the bovine RSV F protein is more toxic than the human RSV F protein. No significant cell loss was observed when gp40-GFP was expressed in MDCK cells. The pan-caspase inhibitor z-VAD (25 μM) significantly reduced the shedding of hF-GFP-expressing cells (Fig. 3B), indicating that this phenomenon is based on F protein-induced apoptosis. Cytoprotection was also achieved when Synagis was added to either the apical or the basolateral chamber of filter-grown cells. The antibody was effective in a concentration-dependent manner; however, concentrations above 5 μg/ml did not further reduce apoptosis (data not shown). A control antibody directed to transforming growth factor β had no protective effect (data not shown).

F protein-induced apoptosis and shedding of epithelial cells was expected to reduce the proportion of F-GFP-expressing cells in the monolayer. To test this idea, the filter-grown cells were treated with trypsin at different times after the induction of F-GFP expression and analyzed by flow cytometry. We observed that the proportion of cells positive for hF-GFP declined in the monolayer from 72% at 24 h to 36% at 72 h

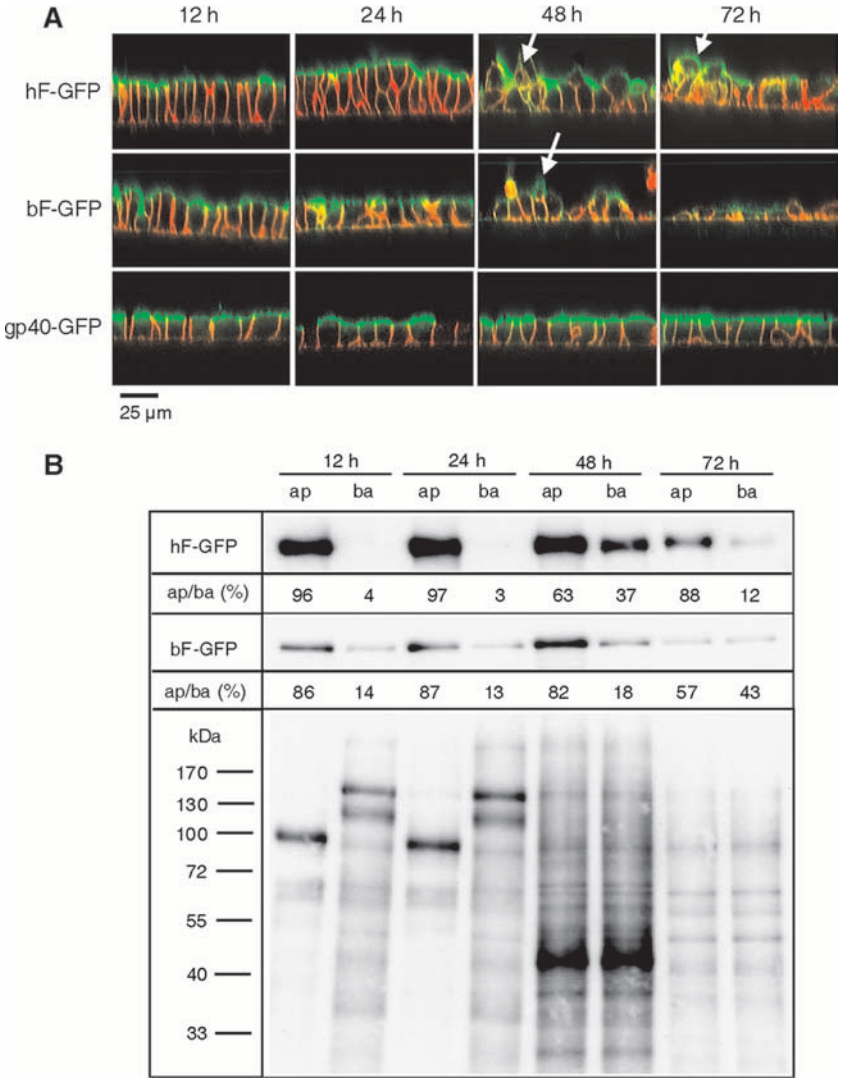

FIG. 2. Conditional expression and localization of GFP-tagged RSV F protein in polarized epithelial MDCK cells. Transgenic MDCK cells were grown on porous filter supports for 3 days prior to the induction of either bF-GFP, hF-GFP, or gp40-GFP. (A) At the indicated times postinduction, cells were stained with a monoclonal antibody directed to β-catenin (red fluorescence) and analyzed by confocal laser scanning microscopy (GFP fluorescence in green). XZ scans of the cells are shown. (B) At the indicated times postinduction of bF-GFP or hF-GFP expression, cell surface proteins of either the apical (ap) or basolateral (ba) plasma membrane were labeled with sulfo-NHS-biotin. F-GFP was immunoprecipitated from cell lysates and analyzed by Western blotting using streptavidin-peroxidase for the detection of biotinylated F-GFP. The amounts of F-GFP were determined by densitometry and the percentages of apical or basolateral F-GFP of total F-GFP (apical plus basolateral F-GFP) were calculated. As a control for biotinylation efficacy, total cell lysates of biotinylated MDCK-(hF-GFP) cells were separated by sodium dodecyl sulfate-polyacrylamide gel electrophoresis, transferred to a nitrocellulose membrane, and probed with streptavidin-peroxidase complex (lower panel).

postinduction (Fig. 3C). In contrast, the proportion of MDCK cells expressing the F protein of Sendai virus with GFP linked to the cytoplasmic domain (SeV-F-GFP) stayed at 85% for the whole time. This viral fusion protein was used as a control because it does not act in an autonomous way like RSV F protein but requires support by the homologous viral attachment protein. RSV F protein-induced cell loss did not result in destruction of the epithelial monolayer. Rather, cells that did not express hF-GFP replaced the extruded cells and restored the monolayer in this way (Fig. 3D).

RSV infection was shown to induce increased epithelial permeability in monolayers of human primary bronchial epithelial cells via induction of the vascular endothelial growth factor, an effect which was inhibited by Synagis (45). Like bronchial epithelial cells, MDCK monolayers set up a measurable TER when grown on porous filter supports for 3 to 4 days (Fig. 3E). This typical parameter of polarized epithelial cells did not change when the cells were induced to express gp40-GFP (not shown) or were grown without induction of an heterologous protein. However, when expression of hF-GFP was induced the TER significantly increased within the first 24 h and then dropped below the initial TER values. At 4 days postinduction of hF-GFP expression, TER was collapsed but subsequently recovered. Interestingly, neither z-VAD nor Synagis had an

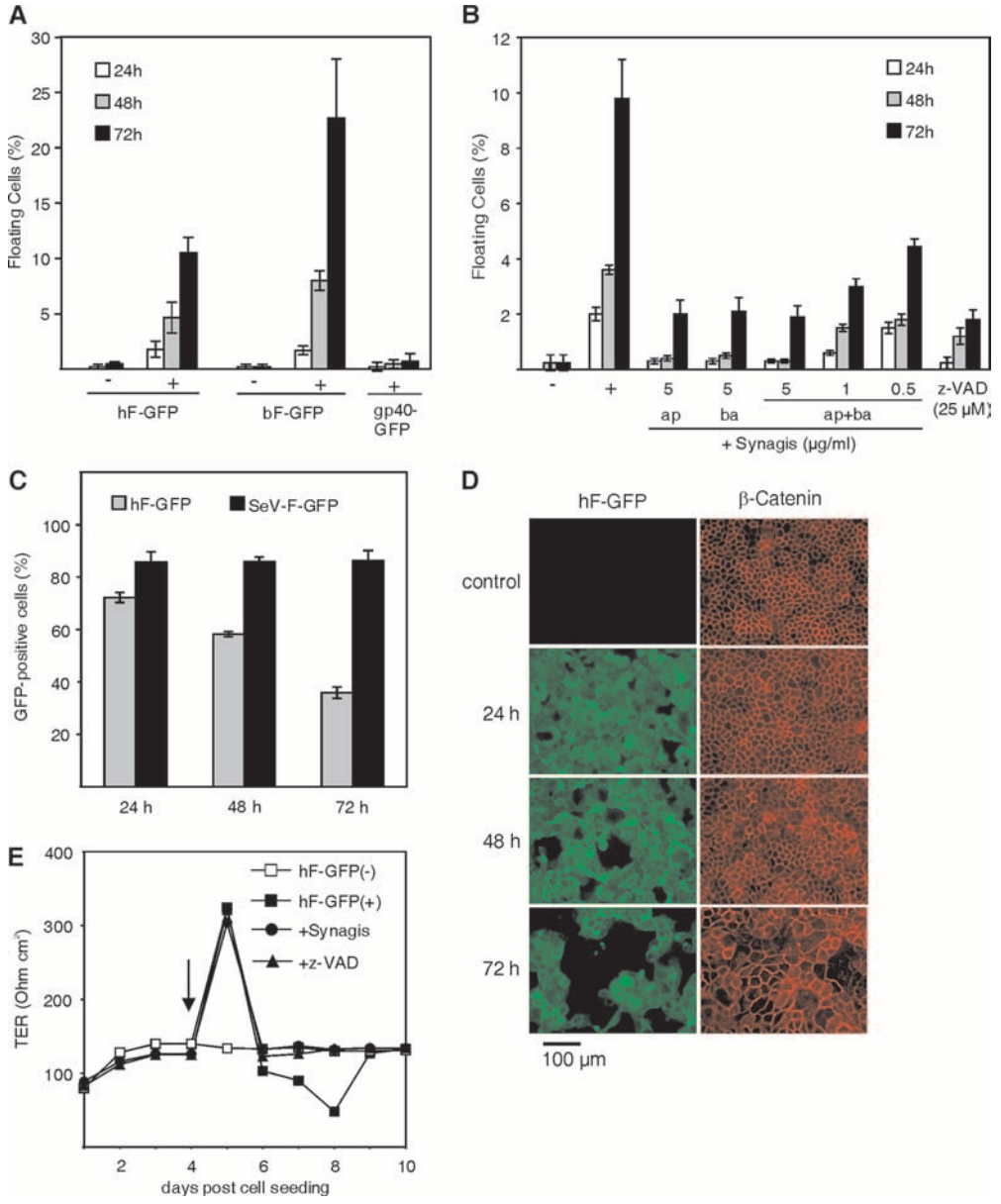

FIG. 3. Impact of RSV F expression on epithelial integrity. MDCK cells were cultured on porous filter supports for 3 days prior to optional induction of gp40-GFP, hF-GFP, and bF-GFP, respectively. (A) The proportion of floating cells in the apical supernatant of MDCK monolayers was determined at the indicated times. The medium was completely replaced every 24 h. (B) The effect of Synagis and pan-caspase inhibitor z-VAD on MDCK cell shedding was determined after induction of hF-GFP expression. Synagis was added to either the apical (ap), basolateral (ba), or to both apical and basolateral (ap+ba) medium of the filter-grown cells. (C) The proportion of GFP-positive cells in MDCK cell monolayers was determined by flow cytometry 24, 48, and 72 h after induction of either hF-GFP or SeV-F-GFP. (D) Restoration of the MDCK monolayer. Filter-grown MDCK cells were fixed at the indicated times after the induction of hF-GFP expression and processed for immunofluorescence analysis of β-catenin. Conventional epifluorescence was performed for detection of hF-GFP (green) and β-catenin (red). (E) Impact of hF-GFP expression on MDCK TER. Transgenic MDCK cells were seeded on porous filter supports, and hF-GFP expression was induced on day 4 (indicated by the arrow). The TER was recorded at daily intervals (solid symbols for induced cells, open symbols for noninduced cells).

effect on the immediate rise of the TER after hF-GFP expression but protected the monolayer from the TER loss afterward. Together, our findings show that expression of RSV F protein in polarized epithelial cells affects cellular polarity, disturbs integrity of the monolayer, and leads to sloughing of epithelial cells in the absence of virus replication.

RSV F promotes apoptosis. To test for the induction of characteristic markers of apoptosis, hF-GFP expression was induced in MDCK cells, and genomic DNA was extracted from floating and adherent cells. The DNA from floating cells revealed the characteristic apoptotic DNA ladder when analyzed by gel electrophoresis (Fig. 4A, lane 3). In contrast, DNA from the adherent fraction of induced cells appeared intact (lane 2), indicating that cells were extruded from the cell monolayer before late apoptotic events became apparent. MDCK cells that were induced to express gp40-GFP did not show any DNA

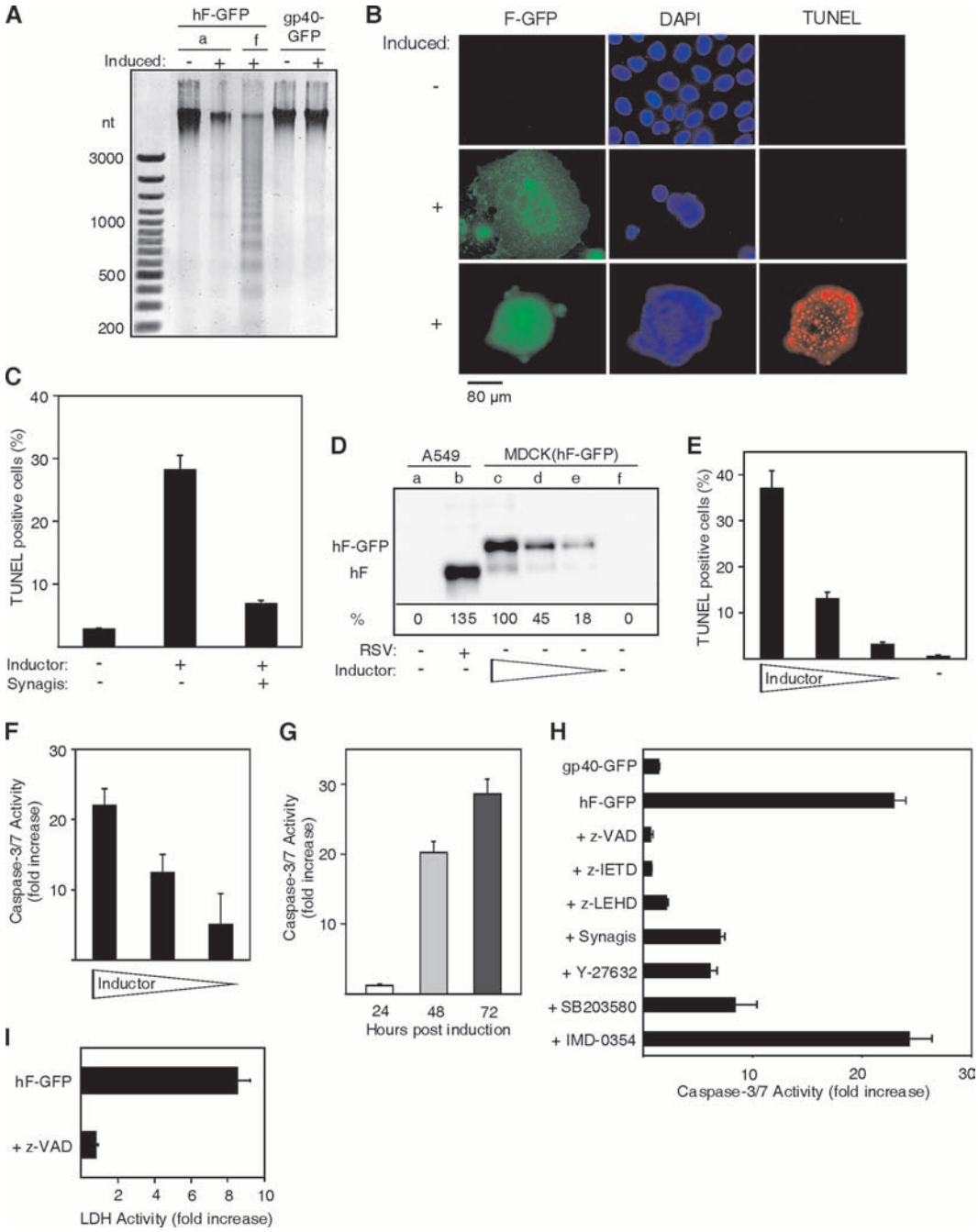

FIG. 4. Analysis of hF-GFP-expressing MDCK cells for apoptotic markers. (A) MDCK cells were induced to express either hF-GFP or gp40-GFP for 48 h or were left uninduced. Genomic DNA was extracted from the adherent (a) and the floating (f) cell fractions of hF-GFP-expressing cells. Cells expressing gp40-GFP did not show any cell loss, and therefore DNA was only extracted from adherent cells. Extracted DNA was separated by gel electrophoresis and visualized by UV light transillumination after ethidium bromide staining. (B) MDCK cells were grown on coverslips for 24 h before hF-GFP expression was induced for 40 h or not induced. The cells were analyzed by fluorescence microscopy after DAPI (blue) or TUNEL (red) staining. GFP fluorescence is shown in green. Note that a large syncytium that was extruded from the monolayer is shown in the lower panels. (C) Expression of hF-GFP was induced for 48 h in the presence or absence of Synagis (5 μg/ml). Adherent and floating cells were pooled and stained with TUNEL reagent. The percentages of positive cells are shown. (D) A549 cells (5×10^5 cells) were infected with RSV A2 using an MOI of 3 PFU/cell, and hF-GFP expression was induced in MDCK cells (5×10^5 cells) using different concentrations of mifepristone (10^{-9} M, 2.5×10^{-10} M, and 0.6×10^{-11} M). After 24 h, the surface proteins of A549 and MDCK cells were labeled with sulfo-NHS-LC-biotin, and F protein was immunoprecipitated from the cell lysates. Biotinylated F protein was detected by Western blotting using streptavidin-peroxidase as probe. The levels of F antigen were quantified by densitometry and are expressed as percentages of the amount of F antigen induced by 10^{-9} M mifepristone. (E) The expression of hF-GFP was induced with different concentrations of mifepristone (see above). Adherent and floating cells were collected 48 h postinduction and stained with TUNEL reagent. The percentages of cells that reacted with the reagent are shown. (F) The caspase-3/7 activity was determined in MDCK cell lysates 48 h after induction of hF-GFP expression using different mifepristone concentrations (see above). (G) The caspase-3/7 activity was determined in cell lysates 24, 48, and 72 h after induction of hF-GFP with 10^{-9} M mifepristone. (H) MDCK cells were induced to express either gp40-GFP or hF-GFP for 40 h in the presence

fragmentation. When the cells were analyzed by immunofluorescence 48 h after the induction of F protein expression, the appearance of syncytia with multiple nuclei in their center was observed (Fig. 4B). Most of these polykaryons contained intact nuclei, as indicated by DNA staining with DAPI, and were negative in the TUNEL assay. However, syncytia that had already detached from the monolayer showed DNA fragmentation and membrane blebbing and were positive in the TUNEL assay (lower panel). At 48 h postinduction of F protein expression, ca. 28% of the total cell population were stained by the TUNEL reagent (Fig. 4C). However, in the presence of Synagis the proportion of TUNEL-positive cells was reduced to 7%. Regularly, mifepristone at 10^{-9} M was used to induce F protein expression in MDCK cells. By this means, F protein expression levels were achieved that were nearly as high as in RSV-infected A549 cells (Fig. 4D). When less mifepristone was used, the expression levels of F protein declined (Fig. 4D) and fewer TUNEL-positive cells were observed (Fig. 4E), indicating that the amount of F protein correlates with the induction of apoptosis.

The effector caspase-3 plays a central role in apoptosis by mediating cleavage and breakdown of several cellular components related to DNA repair and regulation. Caspase-3/7 activity increased more than 20-fold in MDCK cells when hF-GFP expression was induced (Fig. 4F). This increase in caspase-3/7 activity correlated with the amount of F protein expressed (compare Fig. 4F to Fig. 4D). When the caspase-3/7 activity was determined 24 h after hF-GFP induction, no significant increase in activity compared to noninduced cells was detectable (Fig. 4G). However, at days 2 and 3 a dramatic increase in caspase-3/7 activity was observed. The pan-caspase inhibitor z-VAD (25 μM) completely abolished caspase-3/7 activity (Fig. 4H). Inhibitors of caspase-8 and caspase-9 (25 μM) were also effective, suggesting that both initiator caspases are components of a cascade leading to activation of caspase-3/7. Synagis significantly reduced but did not completely abolish caspase-3/7 activation. The antibody had no effect on staurosporine-induced caspase-3/7 activation and cell death (data not shown). Significant inhibition of caspase-3/7 activation was also achieved with both the Rho kinase inhibitor Y-27632 (5 μM) and the p38 mitogen-activated protein kinase (MAPK) inhibitor SB203580 (5 μM), whereas an inhibitor of IκB kinase IMD-0354 (1 μM) had no cytoprotective effect. A higher caspase-3/7 activity was associated with shed cells than with adherent cells (data not shown), indicating that apoptosis became fully apparent only after cells had been extruded from the cell monolayer. A significant increase in LDH activity was detected in the supernatant of MDCK cells 48 h after the induction of hF-GFP expression (Fig. 4I). This effect was completely abolished by pan-caspase inhibitor z-VAD, indicating that the cells were subject to secondary necrosis.

Transcription factor p53 is involved in RSV F-triggered apoptosis. To elucidate whether RSV F-triggered apoptosis requires transcriptional activity, luciferase reporter constructs with promoter elements responding to five different transcription factors were used to transfect MDCK cells. Changes in transcriptional activity were analyzed as a function of conditional hF-GFP expression. This approach revealed that only p53 was activated when hF-GFP expression was induced (Fig. 5A). In contrast, no changes in p53 transcriptional activity were detected after conditional expression of gp40-GFP. Activation of p53-dependent transcription was completely abolished if the MDCK cells had been stably transfected with a dominant-negative p53 (Fig. 5B; p53-DN). The antibody Synagis, the Rho kinase inhibitor Y-27632, and the p38 MAPK inhibitor SB203580 also efficiently reduced p53-dependent reporter expression.

A number of protein kinases can phosphorylate p53 at specific sites, resulting in stabilization and/or activation of this transcription factor. The overall homology between canine and human p53 is relatively high, but there are also important differences. For example, canine p53 lacks serines at positions 9 and 46, and the phosphorylation of the latter in human p53 has been shown to be important for the induction of apoptosis (60). Other phosphorylation sites (serines 6, 37, and 392) are flanked by nonconserved amino acid residues so that phospho-specific antibodies directed to human p53 were not expected to react with the corresponding canine counterparts. However, serine-15 and flanking sequences are highly conserved in both canine and human p53. When a monoclonal antibody reacting with phosphorylated serine-15 of human p53 was used for immunofluorescence analysis of MDCK cells, we observed a strong nuclear signal after induction of hF-GFP (Fig. 5C). The same antibody did not stain the nuclei of MDCK cells after the induction of gp40-GFP expression.

Bax is a p53-regulated proapoptotic protein of the bcl-2 family. Upon activation it undergoes a conformational change and translocates from the cytosol to mitochondria. Bax mediates permeabilization of mitochondrial membranes, resulting in the release of apoptogenic proteins such as cytochrome *c* (73). Using the conformation-dependent antibody N-20 directed against the NH_2 terminus of Bax (19), activated Bax was detected in MDCK cells only if RSV F protein expression was induced (Fig. 5D). The cells displayed a punctate and sometimes vermicular immunostaining pattern indicative of Bax association with mitochondria. All of these findings indicate that the RSV F protein triggers activation of the transcription factor p53, which in turn results in upregulation and/or activation of p53-regulated proapoptotic proteins such as Bax.

To address the question whether p53 activation is responsible for RSV F-induced apoptosis, dominant-negative p53 was stably expressed in MDCK-hF-GFP cells. In these cells,

or absence of the indicated inhibitors (z-VAD, z-IETD, and z-LEHD at 25 μM; Synagis at 5 μg/ml; Y-27632 at 5 μM; SB203580 at 5 μM; or IMD-0354 at 1 μM), and the caspase-3/7 activity was determined in cell lysates. (I) The release of LDH activity was determined 40 h postinduction of hF-GFP in the absence or presence of pan-caspase inhibitor z-VAD (25 μM). The measurement results shown in panels G, H, and I are expressed as the relative fold increase of enzyme activity compared to noninduced cells. Arithmetic means and standard deviations of three experiments are shown.

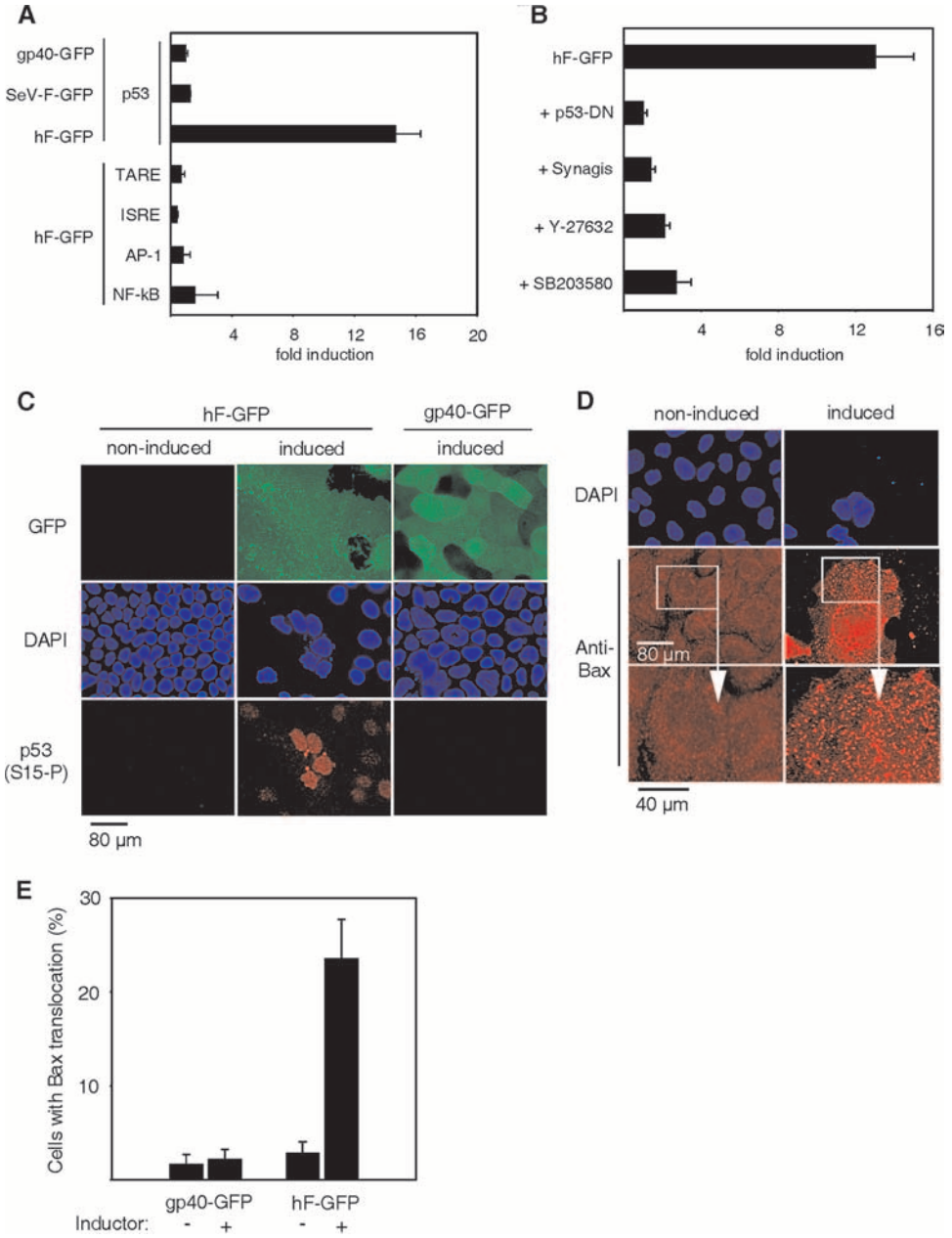

FIG. 5. Activation of p53 transcriptional activity. (A) Transcription factor profiling in MDCK cells expressing hF-GFP. MDCK cells were transfected with luciferase reporter constructs placed under the control of the indicated transcription factors. The luciferase activity was measured in cell lysates 24 h after hF-GFP expression was either induced or not induced. (B) Effect of inhibitors on hF-GFP-triggered p53 activation. MDCK cells with or without stable p53-DN expression were transfected with a p53-controlled luciferase reporter construct. The luciferase activity was determined 24 h after the expression of hF-GFP was induced (or not induced) in the presence or absence of either Synagis (5 μg/ml), Y-27632 (5 μM), or SB203580 (5 μM). (C) Detection of phosphorylated serine-15 of p53. MDCK cells were fixed 40 h after the induction of hF-GFP or gp40-GFP expression and stained for phosphorylated serine-15 of p53, p53(S15-P). Nuclei were counterstained with DAPI. (D) Detection of activated Bax in F-induced polykaryons. MDCK cells were fixed 40 h after the expression of hF-GFP was either not induced (upper panel) or induced (lower panel) and stained with antibody N-20 recognizing activated Bax. The lower panel shows a section of the cells at higher magnification. (E) The proportion of adherent cells showing Bax translocation was determined (n = 300). Arithmetic means and standard deviations from three experiments are shown.

caspase-3/7 activity (Fig. 6A) and cell shedding (Fig. 6B) were significantly lower than in control cells that had been stably transfected with the control vector. Next, we analyzed whether p53 plays a role in apoptosis of A549 cells after infection with RSV. To address this, we generated stable A549 cell clones expressing either p53-DN or p53-specific small hairpin RNA (siRNA-p53). The cells were infected with RSV A2 (3 PFU/cell), and the caspase-3/7 activity was determined 40 h postinfection (Fig. 6C). Infection of A549 cells that had been stably transfected with the control plasmids, either pIRESneo or

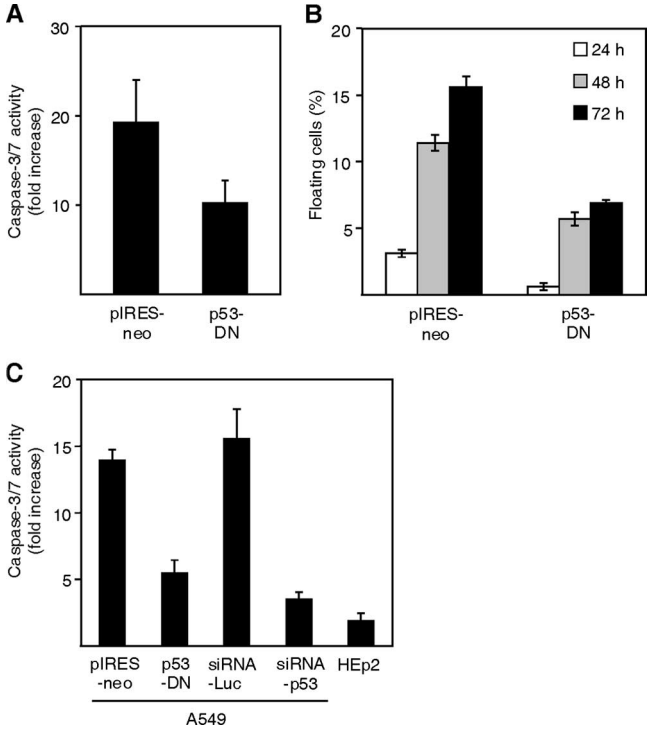

FIG. 6. Importance of p53 for RSV F-triggered apoptosis. (A) MDCK cells were stably transfected with empty pIRESneo plasmid or recombinant plasmid driving the expression of dominant-negative p53 (p53-DN). Caspase-3/7 activity was determined 40 h after induction of hF-GFP, and measurement results were expressed as the relative fold increase of enzyme activity compared to noninduced cells. (B) The proportion of cells shed into the cell culture supernatant was determined at the indicated times after induction of hF-GFP. The medium was completely replaced every 24 h. Arithmetic means and standard deviations of three experiments are shown. (C) HEp2 cells and A549 cells stably transfected with the indicated plasmids were infected with human RSV (A2) using 3 PFU/cell. The relative fold increase of caspase-3/7 activity was determined 40 h postinfection. Arithmetic means and standard deviations of three experiments are shown.

psiRNA-Luc, showed increased caspase-3/7 activities compared to mock-infected cells. In contrast, A549 cells stably transfected with either p53-DN or siRNA-p53 revealed significantly reduced caspase-3/7 activities after infection with RSV.

The human cancer cell line HEp-2 is positive for the human papillomavirus E6 oncogene, which causes ubiquitination and degradation of p53 (81). Although more than 90% of HEp-2 cells became infected with RSV when an MOI of 3 PFU per cell was used (data not shown), only a small increase in caspase-3/7 activity was detected, a finding which is in accordance with published data (50). These findings provide good evidence that p53 is involved in RSV F-induced apoptosis in A549 and MDCK cells.

DISCUSSION

RSV F protein-induced apoptosis. Previous studies provided evidence that primary human airway epithelial cells (50), as well as the human lung epithelial cell line A549 (4, 50, 61), undergo programmed cell death after infection with RSV. We followed up these studies and showed that RSV-mediated apoptosis of epithelial cells was significantly reduced if Synagis, a humanized monoclonal antibody directed to RSV F, was given postinfection. In addition, individual expression of F protein triggered apoptosis in polarized MDCK cells, which were largely protected from cell death in the presence of Synagis. The protective effect of Synagis might be attributed to the ability of this antibody to interfere with the fusion activity of the viral protein. However, it cannot be excluded that Synagis also affects the binding of F protein to an unknown cellular receptor which triggers signaling transduction pathways, leading to programmed cell death. Even though the mechanism of F protein-mediated cytotoxicity have to be dissected in future, it is evident from the present study that the F protein is a major apoptosis-inducing protein of RSV. As a first attempt to identify other proapoptotic RSV proteins, we generated stably transfected MDCK cell clones expressing the BRSV SH protein in a regulated manner. In addition, MDCK cells constitutively expressing the BRSV G protein were generated. However, in neither case did these viral glycoproteins induce apoptosis on their own (unpublished results). This does not rule out that other viral factors may contribute to RSV-mediated cell death.

RSV F protein was found to induce syncytium formation in MDCK monolayers, and these polykaryons were ultimately destined for apoptosis. In addition, we showed that F protein-induced apoptosis is based on activation of the transcription factor and tumor suppressor p53, which could be significantly reduced by inhibiting either p38 MAPK or Rho kinase. F-induced apoptosis was brought down by a factor of 2 when dominant-negative p53 was expressed. The dominant-negative mutation R273H affects the DNA binding and transcriptional activities of p53. However, p53 has been reported to exert transcription-independent proapoptotic functions (36, 48).

Therefore, it is not expected that p53-DN can totally block p53-dependent apoptosis. In accordance with this view, downregulation of p53 by either shRNA or E6 transformation was more efficient than p53-DN in reducing F-induced apoptosis.

In some aspects RSV F protein-mediated cell death is reminiscent of syncytial apoptosis induced by the human immunodeficiency virus type 1 (HIV-1) glycoprotein Env (24, 67, 76). Fusion of HIV-1 Env-expressing cells with cells expressing both the CD4 receptor and the CXCR4 coreceptor results in syncytia which undergo apoptosis after fusion of their nuclei (karyogamy). Nuclear fusion is believed to result from an abortive entry into the prophase of mitosis stimulated by the transient activation of the cyclin-dependent kinase 1(Cdk1), which leads to permeabilization of the nuclear envelope and nuclear accumulation of mammalian target of rapamycin (mTOR) (11). Subsequent phosphorylation and activation of p53 by mTOR and p38 MAPK leads to p53-dependent transcription of proapoptotic proteins such as PUMA and Bax and activation of the mitochondrial pathway of apoptosis.

It has been previously shown that RhoA signaling is important for RSV-induced syncytium formation and that Rho kinase is an important effector in this context (30). Likewise, expression of dominant-negative RhoA has been shown to inhibit HIV-1 envelope fusion with target cell membranes (18). Thus, it is likely that Rho kinase inhibitor Y-27632 was effective in lessening apoptosis by interfering with F protein-mediated syncytium formation. However, Y-27632 may also inhibit other activities of Rho kinase that may be important for F-induced apoptosis. For example, it was shown that RhoA/Rho kinase upregulates Bax to activate a mitochondrial pathway of apoptosis in cardiomyocytes (17). Furthermore, Y-27632 inhibits actin- and myosin-dependent extrusion of preapoptotic cells from epithelial monolayers (69). In this way, Y-27632 may interfere with the full outcome of apoptosis. Rho signaling is also known to be involved in cell cycle progress by suppressing CDK inhibitory protein $p21^{waf/cip}$ and activating cyclins, respectively (52). In syncytia, however, activation of these pathways may lead to an abortive entry into mitosis and subsequent apoptosis or mitotic catastrophe (12). It is noteworthy in this context that RSV infection results in the activation of epidermal growth factor receptor and extracellular-related kinases (57, 58, 65).

The fusion activity of RSV F may not only mediate apoptosis through the formation of syncytia. Viral fusion proteins can also mediate a transient lipid transfer between the outer leaflets of two membranes, a process known as hemifusion. For HIV-1 Env it has been demonstrated that hemifusion is sufficient to trigger apoptosis of target cells (6, 29). Future studies will show whether this mechanism is also true for RSV F protein. In contrast to soluble HIV-1 Env, which induces apoptosis in a number of cell types (67), soluble RSV F protein lacking the transmembrane and cytoplasmic domains did not induce any cytotoxic effects in stably transfected MDCK cells, indicating that association of RSV F protein with the plasma membrane is required for the induction of apoptosis (M. Lorek and G. Zimmer, unpublished results).

Regulation of apoptosis. Early apoptosis is probably detrimental for efficient virus replication. Therefore, it is not surprising that RSV makes use of multiple strategies to delay apoptosis (5, 21, 26, 50, 53, 58, 80). Interestingly, RSV was recently shown to decrease transcription factor p53 to prolong cell survival (33). This is in line with our observation that apoptosis is reduced in A549 cells that express either dominant-negative p53 or p53-specific small hairpin RNA. An additional mechanism that prevents early apoptosis may be attributed to the polarized distribution of the RSV F protein in epithelial cells. The apical transport appears to be an intrinsic property of the F protein and meets the requirements for apical RSV budding (7, 68), but it also guarantees that F protein does not come into contact with the lateral membrane of adjacent cells so that cell-cell fusion and consequent apoptosis is avoided. In accordance with this idea, we found that filter-grown MDCK cells that had established a polarized monolayer were more resistant to F-induced apoptosis than MDCK cells that were not fully polarized because they were grown on cell culture dishes (unpublished results). This concept would also explain why the bovine RSV F protein revealed a higher proapoptotic activity than the human RSV F protein. The latter one was strictly targeted to the apical plasma membrane, while a small fraction of the bovine RSV F protein was also localized at the basolateral domain early after induction. It has been recently suggested that the transmembrane domain is an important determinant for apical transport of the F protein (8). Indeed, the primary sequences of the predicted transmembrane domains reveal some differences between the human and bovine RSV F protein. For example, cysteine 550 in the human RSV F protein is replaced by serine in the bovine RSV F protein (strain Stormond). Cysteine 550 of the human RSV F protein was shown to be subject to acylation (2), but the importance of this posttranslational modification for apical transport is not known. The association of the F protein with lipid rafts might be also relevant for apical transport of the protein (71). It has been recently reported that neither the cytoplasmic domain, the membrane anchor, nor fatty acid modification of F protein is important for its association with lipid rafts, suggesting that the ectodomain may be involved (25). However, data provided by others suggested that the cytoplasmic domain might be involved in lipid raft association (62). Future studies using chimeric proteins must show which domain of the F protein is actually involved in polarized transport and induction of apoptosis. Despite its predominant apical localization, the human RSV F protein ultimately triggered apoptosis of polarized MDCK cells. It is possible that the F protein eventually affects cell polarity by activating RhoA (31), a regulator of epithelial barrier function (9, 43).

While early apoptosis is probably harmful, RSV may benefit from apoptosis late in the replication cycle. Infected cells normally release only low numbers of progeny RSV into the supernatant. However, RSV may stay for some time in the airway lumen while associated with extruded apoptotic cells. Cough may then result in sputum of infectious cellular material and transmission of RSV to other persons. In addition, RSV may be shielded from immune recognition and attack in the airway lumen. Finally, transient loss of epithelial barrier function may allow RSV to spread into extrapulmonary organs as recently suggested (22).

Obstructive bronchitis. Necropsy studies revealed that RSV infection causes sloughing of epithelial cells which aggregate and form plugs along with mucin, fibrin, and inflammatory cells (1, 42, 66). These plugs likely contribute to obstruction of the

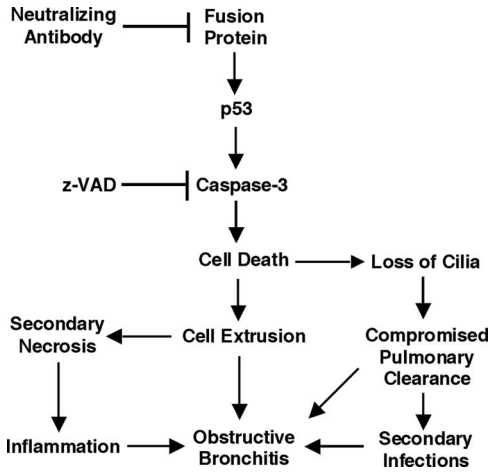

FIG. 7. Proposed role of F protein in RSV pathogenesis. The F protein activates p53 and induces caspase-dependent apoptosis, which leads to the extrusion of epithelial cells and consequent obstruction of the airways. Possible therapies may be based on pharmaceuticals targeting F protein or downstream effectors such caspase-3/7.

small airways, a major complication after infection of premature and young children with RSV. Experimental RSV infection of fetal human tracheas in organ culture showed that the virus infected a population of ciliated epithelial cells and that infection was associated with syncytium formation and cell degeneration (40). Likewise, in a model of well-differentiated human airway epithelial cells, RSV infection was reported to have profound effects on ciliated cells, leading to ciliostasis and sloughing of cells (83). Our finding that the RSV F protein triggers apoptosis and shedding of epithelial cells might provide a possible explanation for these previous observations. Furthermore, RSV-induced apoptosis may also contribute to airway inflammation, which is frequently observed after RSV infection (59). Under physiological conditions apoptotic cells are rapidly removed from the respiratory tract by phagocytic cells; however, massive apoptosis due to RSV infection might overextend this clearance mechanism, giving way to secondary necrosis with consequent inflammation of the respiratory tract (84). The release of nucleotides from necrotic cells may be also responsible for the inhibition of alveolar fluid clearance by a mechanism involving P2Y receptors (16). Thus, direct damage to the respiratory epithelium by RSV F protein might be a first trigger of a causal chain leading to pathogenesis and disease (Fig. 7).

It was previously shown that epithelial cells destined for apoptosis signal their neighbors to extrude them by an actin- and myosin-dependent mechanism (69). Accordingly, we observed that F-induced syncytia were rapidly extruded from the epithelial monolayer even before late markers of apoptosis became apparent. The extruded cells were replaced by other cells with the consequence that the epithelial monolayer appeared healthy and intact (see Fig. 3D). This mechanism, extrusion of apoptotic cells and subsequent repair of the monolayer, might explain why others were unable to detect obvious cytopathic effects when infecting primary airway epithelial cells with recombinant RSV (88). Infected cells were observed for >3 months in this model of well-differentiated human airway epithelial cells. However, it is not known whether these cells had been infected at the outset and maintained throughout the entire period or whether there was turnover of cells and reinfection of newly differentiated ciliated cells (88).

Consequences for the treatment of RSV-induced disease. Monoclonal antibodies such as palivizumab (Synagis) that interfere with fusion activity of RSV F are already in clinical use for the prophylactic treatment of children at high risk for RSV disease (10). The present study shows that Synagis can significantly reduce F-triggered apoptosis and shedding of polarized epithelial cells. Both apical and basolateral application of the antibody proved to be effective, though the F protein was found to reside predominantly at the apical membrane. The neonatal FcRn receptor has been identified in a number of secretory epithelia, including those of the kidney (47) and lung (77). It can be speculated that receptor-mediated transcytosis of Synagis from the basolateral to the apical pole of the cells allowed the antibody to bind to apical F protein. Alternatively, the antibody got access to the antigen after F-induced RhoA activation (31, 64) and RhoA-dependent modulation of epithelial barrier function. Even high concentrations of the antibody did not completely prevent F-mediated cytotoxic effects. This residual cytotoxicity might be mediated by F protein in intracellular compartments, where it is not accessible for Synagis. Interestingly, endoplasmic reticulum-specific stress-activated caspase-12 has been implicated in the apoptosis of RSV-infected A549 cells (4). It is therefore possible that F protein expression causes an endoplasmic reticulum stress response (39) that also contributes to F-triggered apoptosis.

Postinfection administration of neutralizing anti-F antibodies in animal models showed that RSV titers were significantly reduced, whereas beneficial effects on airway obstruction and clinical course of the disease were not achieved (38, 56). Hence, therapeutic antibodies that are given when the disease is already apparent cannot reverse apoptosis that had already occurred. Small-molecule inhibitors of viral fusion proteins represent a novel strategy to combat virus infection and spread (14). Definitely, fusion inhibitors might be useful to reduce the direct RSV F protein-mediated cytotoxic effects; however, the limitations discussed for neutralizing antibodies probably are also true for these compounds. Since apoptosis plays an important role in a number of lung diseases such as asthma, chronic obstructive bronchitis, respiratory distress syndrome, and pulmonary fibrosis, a therapeutic approach based on modulators of apoptosis is currently being discussed (20). Our findings suggest that a similar approach might be useful for the treatment of RSV-induced obstructive bronchitis.

Vaccines based on formalin-inactivated RSV failed to protect children from RSV infection and disease but rather were associated with immunopathological effects (13, 27, 44, 46). Therefore, numerous attempts have been made to generate live attenuated RSV vaccines in the last couple of years (15). However, it turned out that most vaccine candidates were either overattenuated or still too pathogenic for use in children. The F protein may provide an explanation for these difficulties. On the one hand, fusion activity is essential for RSV replication; on the other hand, fusion activity contributes to RSV pathogenesis by triggering apoptosis and sloughing of epithelial cells. Hence, the attenuation of RSV might be only achieved at the expense of effective virus replication and im-

munogenicity. Vector vaccines expressing fusion-incompetent RSV F protein might be superior to live attenuated RSV. However, we may encounter similar problems as before if these vector vaccines are based on enveloped viruses with a pH-independent fusion activity (35, 78), in particular if they are used for mucosal immunization.

ACKNOWLEDGMENTS

The project was supported by grants from the Deutsche Forschungsgemeinschaft to G.Z. (ZI 558/2–2, GRK 745, and SFB 587).

We thank Matthias Dobbelstein and Takashi Fujita for providing plasmids.

REFERENCES

1. **Aherne, W., T. Bird, Court, S. D., P. S. Gardner, and J. McQuillin.** 1970. Pathological changes in virus infections of the lower respiratory tract in children. J. Clin. Pathol. **23:**7–18.
2. **Arumugham, R. G., R. C. Seid, Jr., S. Doyle, S. W. Hildreth, and P. R. Paradiso.** 1989. Fatty acid acylation of the fusion glycoprotein of human respiratory syncytial virus. J. Biol. Chem. **264:**10339–10342.
3. **Barton, T. D., and E. A. Blumberg.** 2005. Viral pneumonias other than cytomegalovirus in transplant recipients. Clin. Chest Med. **26:**707–720, viii.
4. **Bitko, V., and S. Barik.** 2001. An endoplasmic reticulum-specific stress-activated caspase (caspase-12) is implicated in the apoptosis of A549 epithelial cells by respiratory syncytial virus. J. Cell Biochem. **80:**441–454.
5. **Bitko, V., O. Shulyayeva, B. Mazumder, A. Musiyenko, M. Ramaswamy, D. C. Look, and S. Barik.** 2007. Nonstructural proteins of respiratory syncytial virus suppress premature apoptosis by an NF-κB-dependent, interferon-independent mechanism and facilitate virus growth. J. Virol. **81:**1786–1795.
6. **Blanco, J., J. Barretina, K. F. Ferri, E. Jacotot, A. Gutierrez, M. Armand-Ugon, C. Cabrera, G. Kroemer, B. Clotet, and J. A. Este.** 2003. Cell-surface-expressed HIV-1 envelope induces the death of CD4 T cells during GP41-mediated hemifusion-like events. Virology **305:**318–329.
7. **Brock, S. C., J. R. Goldenring, and J. E. Crowe, Jr.** 2003. Apical recycling systems regulate directional budding of respiratory syncytial virus from polarized epithelial cells. Proc. Natl. Acad. Sci. USA **100:**15143–15148.
8. **Brock, S. C., J. M. Heck, P. A. McGraw, and J. E. Crowe, Jr.** 2005. The transmembrane domain of the respiratory syncytial virus F protein is an orientation-independent apical plasma membrane sorting sequence. J. Virol. **79:**12528–12535.
9. **Bruewer, M., A. M. Hopkins, M. E. Hobert, A. Nusrat, and J. L. Madara.** 2004. RhoA, Rac1, and Cdc42 exert distinct effects on epithelial barrier via selective structural and biochemical modulation of junctional proteins and F-actin. Am. J. Physiol. Cell Physiol. **287:**C327–C335.
10. **Cardenas, S., A. Auais, and G. Piedimonte.** 2005. Palivizumab in the prophylaxis of respiratory syncytial virus infection. Expert Rev. Anti. Infect. Ther. **3:**719–726.
11. **Castedo, M., K. F. Ferri, J. Blanco, T. Roumier, N. Larochette, J. Barretina, A. Amendola, R. Nardacci, D. Metivier, J. A. Este, M. Piacentini, and G. Kroemer.** 2001. Human immunodeficiency virus 1 envelope glycoprotein complex-induced apoptosis involves mammalian target of rapamycin/FKBP12-rapamycin-associated protein-mediated p53 phosphorylation. J. Exp. Med. **194:**1097–1110.
12. **Castedo, M., J. L. Perfettini, T. Roumier, K. Andreau, R. Medema, and G. Kroemer.** 2004. Cell death by mitotic catastrophe: a molecular definition. Oncogene **23:**2825–2837.
13. **Chin, J., R. L. Magoffin, L. A. Shearer, J. H. Schieble, and E. H. Lennette.** 1969. Field evaluation of a respiratory syncytial virus vaccine and a trivalent parainfluenza virus vaccine in a pediatric population. Am. J. Epidemiol. **89:**449–463.
14. **Cianci, C., D. R. Langley, D. D. Dischino, Y. Sun, K. L. Yu, A. Stanley, J. Roach, Z. Li, R. Dalterio, R. Colonno, N. A. Meanwell, and M. Krystal.** 2004. Targeting a binding pocket within the trimer-of-hairpins: small-molecule inhibition of viral fusion. Proc. Natl. Acad. Sci. USA **101:**15046–15051.
15. **Collins, P. L., and B. R. Murphy.** 2005. New generation live vaccines against human respiratory syncytial virus designed by reverse genetics. Proc. Am. Thorac. Soc. **2:**166–173.
16. **Davis, I. C., W. M. Sullender, J. M. Hickman-Davis, J. R. Lindsey, and S. Matalon.** 2004. Nucleotide-mediated inhibition of alveolar fluid clearance in BALB/c mice after respiratory syncytial virus infection. Am. J. Physiol. Lung Cell Mol. Physiol. **286:**L112–L120.
17. **Del Re, D. P., S. Miyamoto, and J. H. Brown.** 2007. RhoA/Rho kinase up-regulate Bax to activate a mitochondrial death pathway and induce cardiomyocyte apoptosis. J. Biol. Chem. **282:**8069–8078.
18. **del Real, G., S. Jimenez-Baranda, E. Mira, R. A. Lacalle, P. Lucas, C. Gomez-Mouton, M. Alegret, J. M. Pena, M. Rodriguez-Zapata, M. Alvarez-Mon, A. Martinez, and S. Manes.** 2004. Statins inhibit HIV-1 infection by down-regulating Rho activity. J. Exp. Med. **200:**541–547.
19. **Desagher, S., A. Osen-Sand, A. Nichols, R. Eskes, S. Montessuit, S. Lauper, K. Maundrell, B. Antonsson, and J. C. Martinou.** 1999. Bid-induced conformational change of Bax is responsible for mitochondrial cytochrome *c* release during apoptosis. J. Cell Biol. **144:**891–901.
20. **de Souza, P. M., and M. A. Lindsay.** 2005. Apoptosis as a therapeutic target for the treatment of lung disease. Curr. Opin. Pharmacol. **5:**232–237.
21. **Domachowske, J. B., C. A. Bonville, A. J. Mortelliti, C. B. Colella, U. Kim, and H. F. Rosenberg.** 2000. Respiratory syncytial virus infection induces expression of the anti-apoptosis gene IEX-1L in human respiratory epithelial cells. J. Infect. Dis. **181:**824–830.
22. **Eisenhut, M.** 2006. Extrapulmonary manifestations of severe respiratory syncytial virus infection: a systematic review. Crit. Care. **10:**R107.
23. **Falsey, A. R., and E. E. Walsh.** 2005. Respiratory syncytial virus infection in elderly adults. Drugs Aging **22:**577–587.
24. **Ferri, K. F., E. Jacotot, M. Geuskens, and G. Kroemer.** 2000. Apoptosis and karyogamy in syncytia induced by the HIV-1-envelope glycoprotein complex. Cell Death. Differ. **7:**1137–1139.
25. **Fleming, E. H., A. A. Kolokoltsov, R. A. Davey, J. E. Nichols, and N. J. Roberts, Jr.** 2006. Respiratory syncytial virus F envelope protein associates with lipid rafts without a requirement for other virus proteins. J. Virol. **80:**12160–12170.
26. **Fuentes, S., K. C. Tran, P. Luthra, M. N. Teng, and B. He.** 2007. Function of the respiratory syncytial virus small hydrophobic protein. J. Virol. **81:**8361–8366.
27. **Fulginiti, V. A., J. J. Eller, O. F. Sieber, J. W. Joyner, M. Minamitani, and G. Meiklejohn.** 1969. Respiratory virus immunization. I. A field trial of two inactivated respiratory virus vaccines; an aqueous trivalent parainfluenza virus vaccine and an alum-precipitated respiratory syncytial virus vaccine. Am. J. Epidemiol. **89:**435–448.
28. **Garcia, D. F., P. W. Hiatt, A. Jewell, S. L. Schoonover, S. G. Cron, M. Riggs, S. Grace, C. M. Oermann, and P. A. Piedra.** 2007. Human metapneumovirus and respiratory syncytial virus infections in older children with cystic fibrosis. Pediatr. Pulmonol. **42:**66–74.
29. **Garg, H., A. Joshi, E. O. Freed, and R. Blumenthal.** 2007. Site-specific mutations in HIV-1 gp41 reveal a correlation between HIV-1-mediated bystander apoptosis and fusion/hemifusion. J. Biol. Chem. **282:**16899–16906.
30. **Gower, T. L., M. K. Pastey, M. E. Peeples, P. L. Collins, L. H. McCurdy, T. K. Hart, A. Guth, T. R. Johnson, and B. S. Graham.** 2005. RhoA signaling is required for respiratory syncytial virus-induced syncytium formation and filamentous virion morphology. J. Virol. **79:**5326–5336.
31. **Gower, T. L., M. E. Peeples, P. L. Collins, and B. S. Graham.** 2001. RhoA is activated during respiratory syncytial virus infection. Virology **283:**188–196.
32. **Griscom, N. T., M. E. Wohl, and J. A. Kirkpatrick, Jr.** 1978. Lower respiratory infections: how infants differ from adults. Radiol. Clin. N. Am. **16:**367–387.
33. **Groskreutz, D. J., M. M. Monick, T. O. Yarovinsky, L. S. Powers, D. E. Quelle, S. M. Varga, D. C. Look, and G. W. Hunninghake.** 2007. Respiratory syncytial virus decreases p53 protein to prolong survival of airway epithelial cells. J. Immunol. **179:**2741–2747.
34. **Hall, C. B., E. E. Walsh, C. E. Long, and K. C. Schnabel.** 1991. Immunity to and frequency of reinfection with respiratory syncytial virus. J. Infect. Dis. **163:**693–698.
35. **Haller, A. A., M. Mitiku, and M. MacPhail.** 2003. Bovine parainfluenza virus type 3 (PIV3) expressing the respiratory syncytial virus (RSV) attachment and fusion proteins protects hamsters from challenge with human PIV3 and RSV. J. Gen. Virol. **84:**2153–2162.
36. **Haupt, Y., S. Rowan, E. Shaulian, K. H. Vousden, and M. Oren.** 1995. Induction of apoptosis in HeLa cells by trans-activation-deficient p53. Genes Dev. **9:**2170–2183.
37. **Haws, C., M. E. Krouse, Y. Xia, D. C. Gruenert, and J. J. Wine.** 1992. CFTR channels in immortalized human airway cells. Am. J. Physiol. **263:**L692–L707.
38. **Haynes, L. M., J. Tonkin, L. J. Anderson, and R. A. Tripp.** 2002. Neutralizing anti-F glycoprotein and anti-substance P antibody treatment effectively reduces infection and inflammation associated with respiratory syncytial virus infection. J. Virol. **76:**6873–6881.
39. **He, B.** 2006. Viruses, endoplasmic reticulum stress, and interferon responses. Cell Death. Differ. **13:**393–403.
40. **Henderson, F. W., S. C. Hu, and A. M. Collier.** 1978. Pathogenesis of respiratory syncytial virus infection in ferret and fetal human tracheas in organ culture. Am. Rev. Respir. Dis. **118:**29–37.
41. **Hogg, J. C., J. Williams, J. B. Richardson, P. T. Macklem, and W. M. Thurlbeck.** 1970. Age as a factor in the distribution of lower-airway conductance and in the pathologic anatomy of obstructive lung disease. N. Engl. J. Med. **282:**1283–1287.
42. **Johnson, J. E., R. A. Gonzales, S. J. Olson, P. F. Wright, and B. S. Graham.** 2007. The histopathology of fatal untreated human respiratory syncytial virus infection. Mod. Pathol. **20:**108–119.
43. **Jou, T. S., E. E. Schneeberger, and W. J. Nelson.** 1998. Structural and functional regulation of tight junctions by RhoA and Rac1 small GTPases. J. Cell Biol. **142:**101–115.
44. **Kapikian, A. Z., R. H. Mitchell, R. M. Chanock, R. A. Shvedoff, and C. E. Stewart.** 1969. An epidemiologic study of altered clinical reactivity to respi-

ratory syncytial (RS) virus infection in children previously vaccinated with an inactivated RS virus vaccine. Am. J. Epidemiol. **89:**405–421.
45. **Kilani, M. M., K. A. Mohammed, N. Nasreen, J. A. Hardwick, M. H. Kaplan, R. S. Tepper, and V. B. Antony.** 2004. Respiratory syncytial virus causes increased bronchial epithelial permeability. Chest **126:**186–191.
46. **Kim, H. W., J. G. Canchola, C. D. Brandt, G. Pyles, R. M. Chanock, K. Jensen, and R. H. Parrott.** 1969. Respiratory syncytial virus disease in infants despite prior administration of antigenic inactivated vaccine. Am. J. Epidemiol. **89:**422–434.
47. **Kobayashi, N., Y. Suzuki, T. Tsuge, K. Okumura, C. Ra, and Y. Tomino.** 2002. FcRn-mediated transcytosis of immunoglobulin G in human renal proximal tubular epithelial cells. Am. J. Physiol. Renal Physiol. **282:**F358–F365.
48. **Kokontis, J. M., A. J. Wagner, M. O'Leary, S. Liao, and N. Hay.** 2001. A transcriptional activation function of p53 is dispensable for and inhibitory of its apoptotic function. Oncogene **20:**659–668.
49. **Konig, P., K. Giesow, K. Schuldt, U. J. Buchholz, and G. M. Keil.** 2004. A novel protein expression strategy using recombinant bovine respiratory syncytial virus (BRSV): modifications of the peptide sequence between the two furin cleavage sites of the BRSV fusion protein yield secreted proteins, but affect processing and function of the BRSV fusion protein. J. Gen. Virol. **85:**1815–1824.
50. **Kotelkin, A., E. A. Prikhod'ko, J. I. Cohen, P. L. Collins, and A. Bukreyev.** 2003. Respiratory syncytial virus infection sensitizes cells to apoptosis mediated by tumor necrosis factor-related apoptosis-inducing ligand. J. Virol. **77:**9156–9172.
51. **Kurt-Jones, E. A., L. Popova, L. Kwinn, L. M. Haynes, L. P. Jones, R. A. Tripp, E. E. Walsh, M. W. Freeman, D. T. Golenbock, L. J. Anderson, and R. W. Finberg.** 2000. Pattern recognition receptors TLR4 and CD14 mediate response to respiratory syncytial virus. Nat. Immunol. **1:**398–401.
52. **Liberto, M., D. Cobrinik, and A. Minden.** 2002. Rho regulates $p21^{CIP1}$, cyclin D1, and checkpoint control in mammary epithelial cells. Oncogene **21:**1590–1599.
53. **Lindemans, C. A., P. J. Coffer, I. M. Schellens, P. M. de Graaff, J. L. Kimpen, and L. Koenderman.** 2006. Respiratory syncytial virus inhibits granulocyte apoptosis through a phosphatidylinositol 3-kinase and NF-κB-dependent mechanism. J. Immunol. **176:**5529–5537.
54. **Martin, J. G., S. Siddiqui, and M. Hassan.** 2006. Immune responses to viral infections: relevance for asthma. Paediatr. Respir. Rev. **7**(Suppl. 1)**:**S125–S127.
55. **Martin, S. J., C. P. Reutelingsperger, A. J. McGahon, J. A. Rader, R. C. van Schie, D. M. LaFace, and D. R. Green.** 1995. Early redistribution of plasma membrane phosphatidylserine is a general feature of apoptosis regardless of the initiating stimulus: inhibition by overexpression of Bcl-2 and Abl. J. Exp. Med. **182:**1545–1556.
56. **Mejias, A., S. Chavez-Bueno, A. M. Rios, M. F. Aten, B. Raynor, E. Peromingo, P. Soni, K. D. Olsen, P. A. Kiener, A. M. Gomez, H. S. Jafri, and O. Ramilo.** 2005. Comparative effects of two neutralizing anti-respiratory syncytial virus (RSV) monoclonal antibodies in the RSV murine model: time versus potency. Antimicrob. Agents Chemother. **49:**4700–4707.
57. **Monick, M., J. Staber, K. Thomas, and G. Hunninghake.** 2001. Respiratory syncytial virus infection results in activation of multiple protein kinase C isoforms leading to activation of mitogen-activated protein kinase. J. Immunol. **166:**2681–2687.
58. **Monick, M. M., K. Cameron, J. Staber, L. S. Powers, T. O. Yarovinsky, J. G. Koland, and G. W. Hunninghake.** 2005. Activation of the epidermal growth factor receptor by respiratory syncytial virus results in increased inflammation and delayed apoptosis. J. Biol. Chem. **280:**2147–2158.
59. **Moore, M. L., and R. S. Peebles, Jr.** 2006. Respiratory syncytial virus disease mechanisms implicated by human, animal model, and in vitro data facilitate vaccine strategies and new therapeutics. Pharmacol. Ther. **112:**405–424.
60. **Oda, K., H. Arakawa, T. Tanaka, K. Matsuda, C. Tanikawa, T. Mori, H. Nishimori, K. Tamai, T. Tokino, Y. Nakamura, and Y. Taya.** 2000. p53AIP1, a potential mediator of p53-dependent apoptosis, and its regulation by Ser-46-phosphorylated p53. Cell **102:**849–862.
61. **O'Donnell, D. R., L. Milligan, and J. M. Stark.** 1999. Induction of CD95 (Fas) and apoptosis in respiratory epithelial cell cultures following respiratory syncytial virus infection. Virology **257:**198–207.
62. **Oomens, A. G., K. P. Bevis, and G. W. Wertz.** 2006. The cytoplasmic tail of the human respiratory syncytial virus F protein plays critical roles in cellular localization of the F protein and infectious progeny production. J. Virol. **80:**10465–10477.
63. **Openshaw, P. J.** 2002. Potential therapeutic implications of new insights into respiratory syncytial virus disease. Respir. Res. **3**(Suppl. 1)**:**S15–S20.
64. **Pastey, M. K., J. E. Crowe, Jr., and B. S. Graham.** 1999. RhoA interacts with the fusion glycoprotein of respiratory syncytial virus and facilitates virus-induced syncytium formation. J. Virol. **73:**7262–7270.
65. **Pazdrak, K., B. Olszewska-Pazdrak, T. Liu, R. Takizawa, A. R. Brasier, R. P. Garofalo, and A. Casola.** 2002. MAPK activation is involved in posttranscriptional regulation of RSV-induced RANTES gene expression. Am. J. Physiol. Lung Cell Mol. Physiol. **283:**L364–L372.
66. **Peebles, R. S., Jr., and B. S. Graham.** 2005. Pathogenesis of respiratory syncytial virus infection in the murine model. Proc. Am. Thorac. Soc. **2:**110–115.
67. **Perfettini, J. L., M. Castedo, T. Roumier, K. Andreau, R. Nardacci, M. Piacentini, and G. Kroemer.** 2005. Mechanisms of apoptosis induction by the HIV-1 envelope. Cell Death. Differ. **12**(Suppl. 1)**:**916–923.
68. **Roberts, S. R., R. W. Compans, and G. W. Wertz.** 1995. Respiratory syncytial virus matures at the apical surfaces of polarized epithelial cells. J. Virol. **69:**2667–2673.
69. **Rosenblatt, J., M. C. Raff, and L. P. Cramer.** 2001. An epithelial cell destined for apoptosis signals its neighbors to extrude it by an actin- and myosin-dependent mechanism. Curr. Biol. **11:**1847–1857.
70. **Schlender, J., G. Walliser, J. Fricke, and K. K. Conzelmann.** 2002. Respiratory syncytial virus fusion protein mediates inhibition of mitogen-induced T-cell proliferation by contact. J. Virol. **76:**1163–1170.
71. **Schuck, S., and K. Simons.** 2004. Polarized sorting in epithelial cells: raft clustering and the biogenesis of the apical membrane. J. Cell Sci. **117:**5955–5964.
72. **Schwarze, J., D. R. O'Donnell, A. Rohwedder, and P. J. Openshaw.** 2004. Latency and persistence of respiratory syncytial virus despite T-cell immunity. Am. J. Respir. Crit. Care Med. **169:**801–805.
73. **Shen, Y., and E. White.** 2001. p53-dependent apoptosis pathways. Adv. Cancer Res. **82:**55–84.
74. **Sigurs, N., R. Bjarnason, F. Sigurbergsson, and B. Kjellman.** 2000. Respiratory syncytial virus bronchiolitis in infancy is an important risk factor for asthma and allergy at age 7. Am. J. Respir. Crit. Care Med. **161:**1501–1507.
75. **Singleton, R., N. Etchart, S. Hou, and L. Hyland.** 2003. Inability to evoke a long-lasting protective immune response to respiratory syncytial virus infection in mice correlates with ineffective nasal antibody responses. J. Virol. **77:**11303–11311.
76. **Sodroski, J., W. C. Goh, C. Rosen, K. Campbell, and W. A. Haseltine.** 1986. Role of the HTLV-1II/LAV envelope in syncytium formation and cytopathicity. Nature **322:**470–474.
77. **Spiekermann, G. M., P. W. Finn, E. S. Ward, J. Dumont, B. L. Dickinson, R. S. Blumberg, and W. I. Lencer.** 2002. Receptor-mediated immunoglobulin G transport across mucosal barriers in adult life: functional expression of FcRn in the mammalian lung. J. Exp. Med. **196:**303–310.
78. **Tang, R. S., M. MacPhail, J. H. Schickli, J. Kaur, C. L. Robinson, H. A. Lawlor, J. M. Guzzetta, R. R. Spaete, and A. A. Haller.** 2004. Parainfluenza virus type 3 expressing the native or soluble fusion (F) protein of respiratory syncytial virus (RSV) confers protection from RSV infection in African green monkeys. J. Virol. **78:**11198–11207.
79. **Ternette, N., D. Stefanou, S. Kuate, K. Uberla, and T. Grunwald.** 2007. Expression of RNA virus proteins by RNA polymerase II dependent expression plasmids is hindered at multiple steps. Virol. J. **4:**51.
80. **Thomas, K. W., M. M. Monick, J. M. Staber, T. Yarovinsky, A. B. Carter, and G. W. Hunninghake.** 2002. Respiratory syncytial virus inhibits apoptosis and induces NF-κB activity through a phosphatidylinositol 3-kinase-dependent pathway. J. Biol. Chem. **277:**492–501.
81. **Thomas, M., G. Matlashewski, D. Pim, and L. Banks.** 1996. Induction of apoptosis by p53 is independent of its oligomeric state and can be abolished by HPV-18 E6 through ubiquitin mediated degradation. Oncogene **13:**265–273.
82. **Thompson, W. W., D. K. Shay, E. Weintraub, L. Brammer, N. Cox, L. J. Anderson, and K. Fukuda.** 2003. Mortality associated with influenza and respiratory syncytial virus in the United States. JAMA **289:**179–186.
83. **Tristram, D. A., W. Hicks, Jr., and R. Hard.** 1998. Respiratory syncytial virus and human bronchial epithelium. Arch. Otolaryngol. Head Neck Surg. **124:**777–783.
84. **Vandivier, R. W., P. M. Henson, and I. S. Douglas.** 2006. Burying the dead: the impact of failed apoptotic cell removal (efferocytosis) on chronic inflammatory lung disease. Chest **129:**1673–1682.
85. **Wat, D., and I. Doull.** 2003. Respiratory virus infections in cystic fibrosis. Paediatr. Respir. Rev. **4:**172–177.
86. **Yoneyama, M., M. Kikuchi, T. Natsukawa, N. Shinobu, T. Imaizumi, M. Miyagishi, K. Taira, S. Akira, and T. Fujita.** 2004. The RNA helicase RIG-I has an essential function in double-stranded RNA-induced innate antiviral responses. Nat. Immunol. **5:**730–737.
87. **You, D., D. Becnel, K. Wang, M. Ripple, M. Daly, and S. A. Cormier.** 2006. Exposure of neonates to respiratory syncytial virus is critical in determining subsequent airway response in adults. Respir. Res. **7:**107.
88. **Zhang, L., M. E. Peeples, R. C. Boucher, P. L. Collins, and R. J. Pickles.** 2002. Respiratory syncytial virus infection of human airway epithelial cells is polarized, specific to ciliated cells, and without obvious cytopathology. J. Virol. **76:**5654–5666.
89. **Zimmer, G., L. Budz, and G. Herrler.** 2001. Proteolytic activation of respiratory syncytial virus fusion protein. Cleavage at two furin consensus sequences. J. Biol. Chem. **276:**31642–31650.
90. **Zimmer, G., K. K. Conzelmann, and G. Herrler.** 2002. Cleavage at the furin consensus sequence RAR/KR(109) and presence of the intervening peptide of the respiratory syncytial virus fusion protein are dispensable for virus replication in cell culture. J. Virol. **76:**9218–9224.
91. **Zimmer, G., F. Lottspeich, A. Maisner, H. D. Klenk, and G. Herrler.** 1997. Molecular characterization of gp40, a mucin-type glycoprotein from the apical plasma membrane of Madin-Darby canine kidney cells (type I). Biochem. J. **326**(Pt. 1)**:**99–108.